Parametric Representation of Creep Crack Growth Rate

T. HOLLSTEIN
Fraunhofer-Institut für Werkstoffmechanik, D 7800 Freiburg, FRG

ABSTRACT

The creep crack growth behaviour of different steels and alloys is investigated. The materials presented are chosen in order to demonstrate the ability and the limits of various one-parameter fracture mechanics approaches.

Examples are shown where creep crack growth takes place under predominantly elastic conditions, under transient conditions from elastic material behaviour to steady state creep, under steady state creep conditions, partly with transients to time independent plastic material behaviour, or plastic collapse, respectively.

INTRODUCTION

Several one-parameter fracture mechanics approaches for describing crack growth under creep conditions have been developed and investigated during the last 15 years: The general idea of these approaches is that with these parameters, e.g. the stress intensity factor K, the J integral or the C* integral, the crack tip stress and strain fields can be described under certain limiting conditions, and that with these values stable crack growth, and crack growth rate, respectively, can be described, independent of size and geometry of the structure or the specimen.

This independence of geometry leads to the ability to assess defect acceptability at the desing stage to predict (residual) lifetimes of high-temperature components containing (pre-existing) flaws.

The stress and strain fields around a crack tip in elastic nonlinear viscous material have been given by Riedel and Rice (1980). They defined a C(t) function which describes the time and stress dependent amplitude of the singularity of the stresses and the strain rates at a crack tip. Riedel (1987) analysed C(t) for various creep conditions. C(t) can be reduced for the short-time limit of small creep zones to an expression with J which further can be reduced to an expression with K for small plastic zones, i.e. for linear elastic conditions. For the long-time limit (large creep zones extending through the remaining ligament), C(t) approaches the C* integral, defined by Ohji et al. (1974) and Landes et al. (1976).

A characteristic time t_1 dividing the whole time domain into a short-time regime, $t \ll t_1$, and a long-time regime, $t \gg t_1$, was derived by Riedel and Rice (1980):

$$t_1 = \frac{J}{(n+1)\, C^*} \qquad (1)$$

(n = creep exponent in a Norton's type power creep law). For the linear elastic case with negligible instantaneous plasticity, J can be replaced by K^2/E' (E'= Young's modulus). For times $t \ll t_1$, crack growth is controlled by K or J, and for $t \gg t_1$ by C*.

Since many materials under normal loading conditions exhibit creep deformation and crack growth under transients from linear elastic (with small creep zones ahead of a crack tip) to steady-state creep (with creep of the whole ligament) interpolation parameters C_t have been developed for these "non steady state creep conditions", e.g. by Saxena and Landes (1984), Saxena (1986) and Riedel (1987):

$$C_t \approx C(t) = [1+t_1/t+(t_2/t)^{p/(1+p)}] \cdot C^* \qquad (2)$$

Here t_2 is a characteristic time for the transition from primary to secondary creep of the specimen, and p is the hardening exponent for primary creep; often p = 2. Neglecting the effects due to primary creep, $t_2 = 0$, C_t can be expressed by the stress intensity factor K in the short time limit and it reduces to C* in the long time limit.

Another one-parameter description of creep crack growth can be made by P or Q* parameters developed by Yokobori et al. (1980, 1987). Besides these one-parameter approaches for describing creep crack growth, several two-parameter approaches exist. In these "engineering" approaches, the crack tip behaviour is considered in addition to the development of damage in the far field (see Ewald et al., 1985, Webster et al., 1986, Ainsworth et al., 1987).

In this paper, the crack tip characterizing C(t) function - reduced to the special cases K, J, C*, C_t - is considered only.

MATERIALS AND SPECIMENS

Results for five different materials are discussed here. The materials are a 32% Ni 20% Cr steel (Incoloy 800 H), a 18% Cr 11% Ni steel (X6 CrNi 18 11, A 304), a 1% Cr steel (21 CrMoNiV 5 7), a 9% Cr steel and a 22% Cr 12% Co Ni-base alloy (NiCr 22 Co 12 Mo, Inconel 617). The results have been gathered using compact (CT) and tension specimens with centre notches (CN) or part through elliptical surface cracks (PTC). The thickness and the width of the specimens in millimetres are shown in the figures by appending the respective numbers (e.g. CT 25/50). Most of the specimens have been fatigue precracked with a final load lower than the load for the creep crack growth test. The CT specimens have been side grooved (10% of the total thickness at each side) after fatigue precracking.

PARAMETER DETERMINATION

Creep crack growth rates $\dot{a}$ were determined from the crack length versus time records. These were constructed using the output mainly from dc or ac potential drop instrumentation, and in some cases from the single-specimen partial unloading compliance method.

The stress intensity factor K and the J integral were determined according to the ASTM Standards E 399 and E 813, respectively.

C* was determined using the following approximate formula, which is very well suited for experimental application:

$$C^* = \eta_c \frac{F\, \dot{V}_c}{B\,(W-a)} \qquad (3)$$

where F, W, a are force, width of specimen and crack length. The effect of side grooves was taken into account by using an effective specimen thickness for B in eq. (3) according to Shih et al. (1977). $\dot{V}_c$ is the load line displacement rate due to creep only which can be evaluated by subtracting the elastic contribution to the displacement caused by crack growth. η_c is a factor depending on geometry and slightly on creep exponent and relative crack length.

The η_c values used here can be described by (see e.g. Webster, 1983, and Hollstein et al., 1988)

$$\eta_c = \frac{n}{n+1}\left(2 + 0.52\,\frac{W-a}{W}\right) \quad \text{for the CT specimens,} \qquad (4)$$

$$\eta_c = \frac{n}{n+1} \quad \text{for the CN specimens,} \qquad (5)$$

$$\eta_c = 0.17 \quad \text{for the PTC specimens.} \qquad (6)$$

C_t can be evaluated using a simple approximate formula developed by Saxena (1986)

$$C_t = \frac{F\, \dot{V}_c}{B(W-a)} \frac{f'}{f}\,(1-a/W) \qquad (7)$$

where $f = f(a/W) = K/(FB\sqrt{W})$ is the K calibration factor, and $f' = df/d(a/W)$.

Under steady-state creep conditions, C* and C_t should become identical. However, eq. (7) differs numerically from eq. (3) slightly:
For n = 6 and a/W = 0.5, eq. (7) leads to about 20% lower values for CT specimens, and to about 30% higher values for CN specimens, than eq. (3).

C* CONTROLLED CRACK GROWTH

In two of the alloys presented here creep crack growth is controlled by C* for a wide range of loadings. That is shown in Figs. 1 and 2, where the crack growth rates $\dot{a}$ in the austenitic 18% Cr 11% Ni steel and in Incoloy 800 H are plotted vs. C*. The resulting power law correlations are independent of geometry (for the Incoloy 800 H, a tube with an outer circumferential crack loaded under internal pressure plus superimposed tension was also tested, see Rödig et al., 1988), of specimen size and the loading conditions investigated, i.e. F = const. and $\dot{V}$ = const. These correlations hold also for decreasing crack growth rates investigated for X6 CrNi 18 11 (see Hollstein, 1986), and slow cyclic loading conditions investigated for Incoloy 800 H (see Hollstein and Kienzler, 1988).

AFR 2-Z

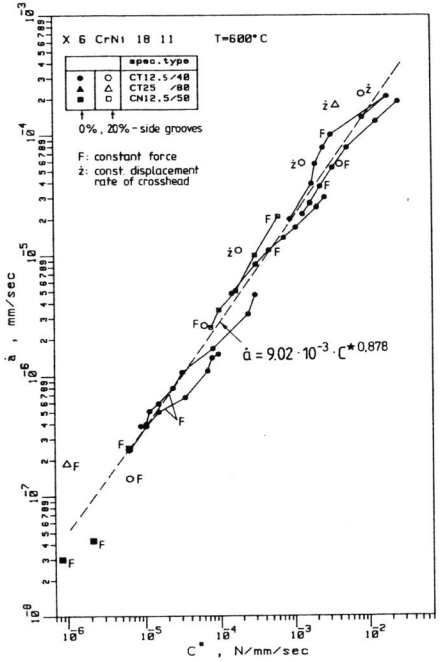

Fig. 1: Creep crack growth rate ȧ as a function of C* for X6 CrNi 18 11

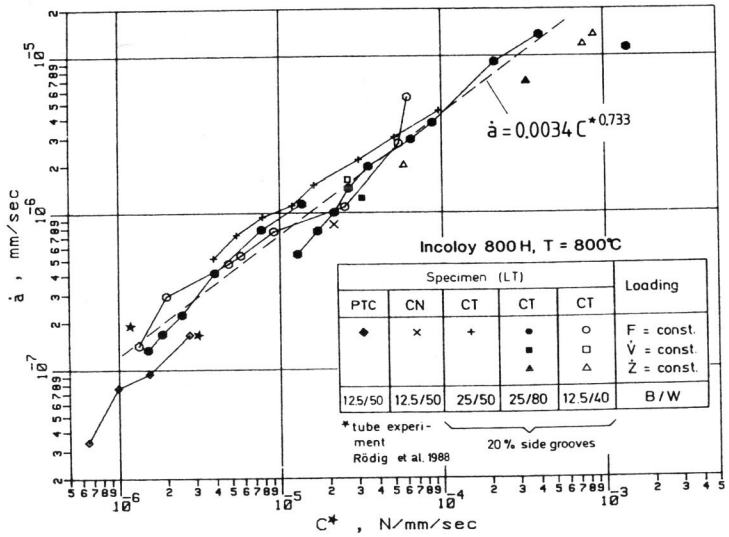

Fig. 2: Creep crack growth rate ȧ as a function of C* for Incoloy 800 H (Ż = constant rate of cross head displacement)

In contrast, if the crack growth rates of the tests in Figs. 1 and 2 are plotted vs. the stress intensity factor K, a difference of several decades in ȧ for different specimen geometries or sizes at an identical K value would appear (Hollstein and Kienzler, 1988).

This behaviour is not unexpected because the transition time t_1, eq. (1), is calculated to be in the range of minutes to a few hours, which is short compared to the testing times and possible specimen lifetime, respectively. This indicates that crack growth occurs under steady-state creep conditions here.

LIMITS OF C* CONTROLLED CRACK GROWTH

Effects of Plasticity, Incoloy 800 H

There are several factors which bound the range of validity of C*. One of them is instantaneous, rate-independent plasticity. Its effect is demonstrated for relatively short-term, constant-displacement rate tests on Incoloy 800 H. For this alloy, slightly different from the previous one, crack growth was determined at 700°C at two different loading rates and also at lower temperatures. Results of these tests are shown in Fig. 3 together with the scatterband of the results of Fig. 2. If the small dependence of C* on temperature for fixed ȧ is not taken into account (points 4,5,6,7 for 400, 500, 600 and 700°C), all values ȧ = f(C*) are well within the same scatterband.

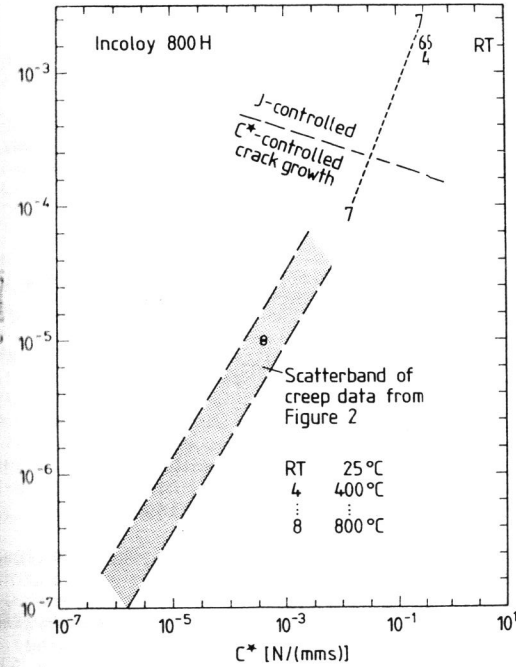

Fig. 3: Limits of C* controlled crack growth

As an intuitive estimate, one would expect that the crack growth for the experiments at temperatures up to 700°C with a loading rate of $\dot{V}$ = 0.25 mm/min (testing time 1.2 h) is J-controlled whereas the crack growth for 700°C with a loading rate of $\dot{V}$ = 0.017 mm/min (testing time 9.6 h) and at 800°C for all other tests is C*-controlled. A limit, based on the transition time t_1, is drawn in Fig. 3. For the tests at 700°C with $\dot{V}$ = 0.017 mm/min, t_1 is of the order of 1 - 2 hours, corresponding to one sixth of the testing time. One can argue that after that time the crack tip stresses have been largely redistributed, and that for longer testing times C* is the characterizing crack tip field parameter while for shorter testing times, J is the relevant parameter.

Small unloadings during the tests support this opinion (see Hollstein and Voss, 1986). For the faster tests, these partial unloadings show large nonlinearities due to stress redistribution whereas for the slower tests no stress redistribution, i.e. time dependent nonlinearity, was apparent.

Effects of Elasticity, 1% Chromium Steel

Fig. 4 shows a plot of the crack growth rate $\dot{a}$ vs. the C* integral for all tested specimens of the 1% Cr steel. Data of the first transient region from the beginning of the test up to the first attainment of a constant crack opening displacement rate $\dot{V}$ have been omitted from Fig. 4. The conclusions which can be drawn are:

1. Within a scatterband of a factor of about $\pm$ 3 the data can be described by a power law.

2. At C* values lower than 10^{-6} N/(mm·s), an indication of some dependence on specimen size (triaxiality) is apparent. Increasing the specimen size corresponds to increasing crack growth rates for the same C* values. The CN specimens without side grooves having the lowest constraint lie significantly below the CT specimens with side grooves, and the CT50/100 specimens having the highes constraint lie at the top of the scatterband. This behaviour has also been found by Kloos et al. (1987) and Ewald et al. (1987) for 1% CrMoV steels.

3. Tails are present in the first part of most of the the tests, covering the greatest fraction of the lifetime. These tails can be explained by a model of Riedel (1987). He derived a correlation

$$\dot{a} \sim C^{*n/n+1} \cdot \Delta a^{1/n+1}, \qquad (8)$$

where the term with the crack growth increment leads to the tails.

4. Results for one of the CT 12.5/40 specimens fall somewhat outside the common scatter-band (at the right side of Fig. 4). This is not surprising, since this specimen was tested within 12 hours. Here, plasticity effects as already discussed in the preceding chapter suggest that a J integral evaluation would be appropriate.

5. Some of the differences may also be explained by a possible crack length dependence, where large specimens with long cracks lead to higher values of $\dot{a}$ (for the same C* values) than smaller specimens with shorter cracks. Such a trend is conceivable if crack growth occurs in the range between K control and C* control. This can be demonstrated by the following argument: Consider a situation in which crack growth occurs in the K-

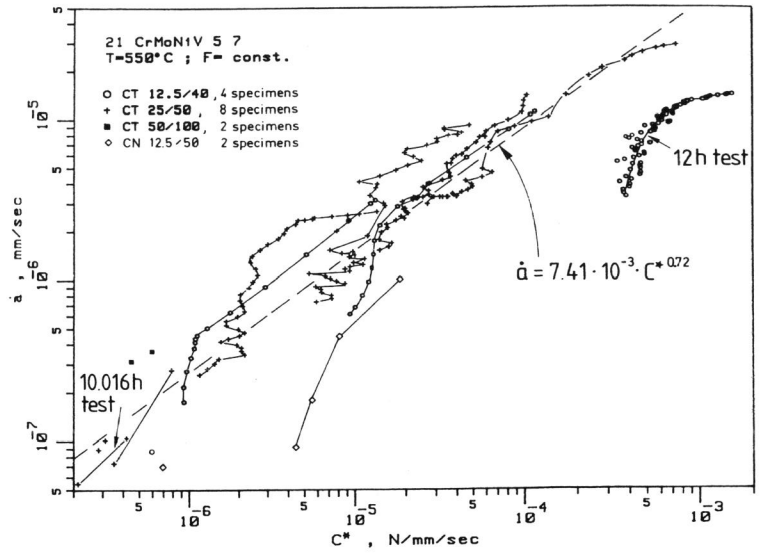

Fig. 4: Creep crack growth rate $\dot{a}$ plotted vs. C* integral; tests from 12 hrs to 10.016 hrs; connected symbols belong to same specimen

controlled regime. For convenience, a power-law relation, $\dot{a} \sim K^m$ is assumed to hold (e.g. Riedel, 1987). If one erroneously tries to use C* in this hypothetical case, one eliminates K by its relation to the applied stress and the crack length, $K \sim \sqrt{a}\,\sigma$, and replaces σ by $C^* \sim a \cdot \sigma^{n+1}$ (Kumar et al., 1981). Then one obtains

$$\dot{a} \sim a^{m/2 - m/(n+1)} \cdot C^{*m/(n+1)} \qquad (9)$$

This shows that, if C* is applied in a case which is actually controlled by K, a dependence on crack length is expected to occur.

Although the tests reported here have not been carried out in the K-controlled regime, elastic contributions to the displacement field cannot be neglected as will be shown next.

In Fig. 5, $\dot{a}$ is plotted versus the stress intensity factor K for the same tests as already shown in Fig. 4. The data at the beginning of the test lie at the lower bound and at the end of the test at the upper bound of the scatterband of all results.

Plotting only the initial values of $\dot{a}$ and K in one diagram (Fig. 6), a very good correlation is found. This indicates that during the first parts of the experiments, where the elastic transients predominate, crack growth rates are correlated by K.

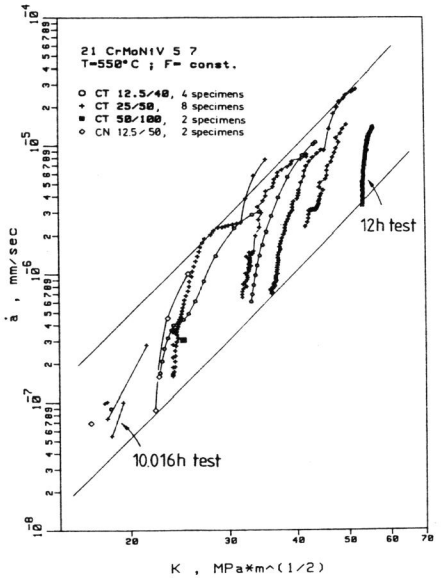

Fig. 5: Creep crack growth rate ȧ plotted vs. stress intensity factor K; connected symbols belong to the same specimen

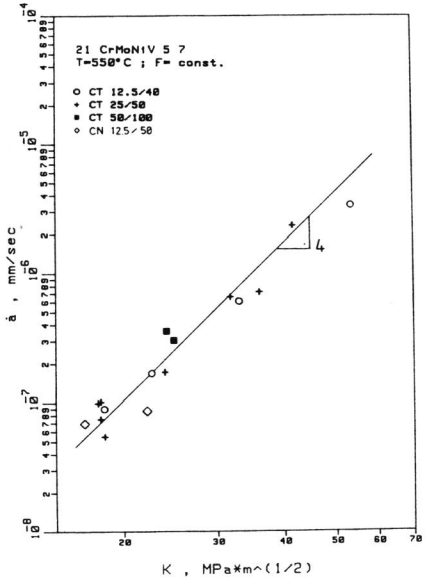

Fig. 6: Initial values of ȧ and K, belonging to the region for first attainment of constant crack opening displacement rate $\dot{V}$

The better correlation, in general, between ȧ and C* than that between ȧ and K is in agreement with the model of Riedel and Rice (1981). Calculating the transition time t_1 according to eq. (1) yields $t_1 \approx 60$ h for ȧ = 10^{-6} mm/s. For times $t \ll t_1$, creep crack growth should be correlated with K, and for $t \gg t_1$ with C*. That means that the creep crack growth rates measured here are influenced by elastic transients.

A conclusion which can be drawn from these experiments is, that independently of geometry, the crack growth rate in the first part of an experiment (as shown for example in Fig. 6) is characterized by K, whereas the crack growth rate towards the end of an experiment with rapidly increasing values of ȧ and $\dot{V}$ is characterized by C*.

An evaluation of the C_t parameter according to Saxena (1986), developed for those non-steady-state creep conditions, leads to similar results since the formulae for C_t and C* calculations are nearly identical.

Limitation to C* due to Crack Tip Blunting, Inconel 617

Results for Inconel 617 at 900°C are shown in Fig. 7. As for the ferritic steel in the previous chapter, only constant or increasing values of C* and ȧ are plotted, corresponding to stationary conditions. The tension specimen with elliptical part-through crack exhibits low values of C* and ȧ. This

happened because for this specimen an unexpectedly low η_c value of 0.17 - necessary for C* evaluation according to eq. (3) - was determined by a three-dimensional finite element analysis only during the course of the experiment.

Two features are obvious from Fig. 7: At first the data can be described by a power law disregarding the behaviour of the CN specimens. Secondly, constant crack growth rates are found for increasing C* values for the two CN specimens tested. This indicates that the stresses and strain rates at the crack tips in the CN specimens cannot be described any longer by C*. This

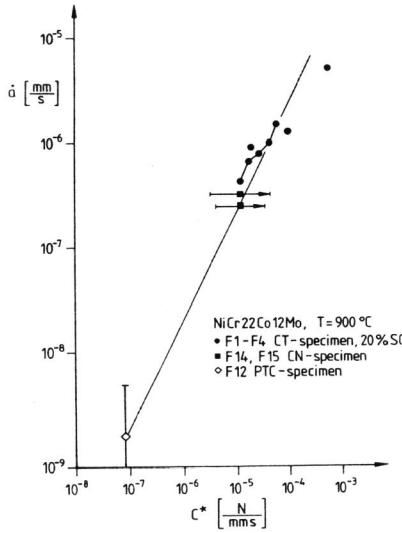

Fig. 7: Creep crack growth rate ȧ as a function of C*

may be due to too large crack tip blunting δ_t. If δ_t is calculated according to Riedel (1987)

$$\delta_t \approx A^{1/n} \cdot C^* \cdot t^{(n+1)/n} \qquad (10)$$

one gets after an initiation time t_i of about 40 h, determined by Hollstein and Kienzler (1987) and for C* = $2 \cdot 10^{-5}$ N/(mm·s) $\delta_t \approx 0.04$ mm.

Inserting this value in a validity criterion for the existence of a unique asymptotic crack tip field (see e.g. Riedel, 1987)

$$a, (W-a) \approx 2\, M\, \delta_t \qquad (11)$$

(M = 25 for CT and 200 for CN specimens), yields for the right-hand side of eq. (11), 2 mm for T and 16 mm for CN specimens. Hence, eq. (11) is fulfilled for CT but violated for CN specimens. This means that C* cannot be applied to the tests with CN specimens because of pronounced crack-tip blunting.

K-CONTROLLED CRACK GROWTH ?

The crack growth rates for the tests of the 9% Cr material at 600°C are plotted as functions of K and C*, in Figs. 8a and 8b, respectively.

The data at 600°C lie in the same scatter band as those determined by Hollstein and Gnirss (1985) for a service exposed 12%-chromium-steel weld joint at 550°C. The K/$\dot{a}$ values are similar to those from Speidel (1982) for a 12% chromium steel at 550°C and 600°C. The data are correlated better to the stress intensity factor K than to the C* integral. The transition time t_1 according to eq. (1) is in the order of some hundred hours and thereby larger than for comparative situations of the 1% Cr steel discussed earlier, and in the order of the specimens' testing time . So, it is not possible to decide from eq. (1) whether the crack growth rate is correlated with K or with C* for these experiments. Specimens with other geometries and sizes have to clarify this situation.

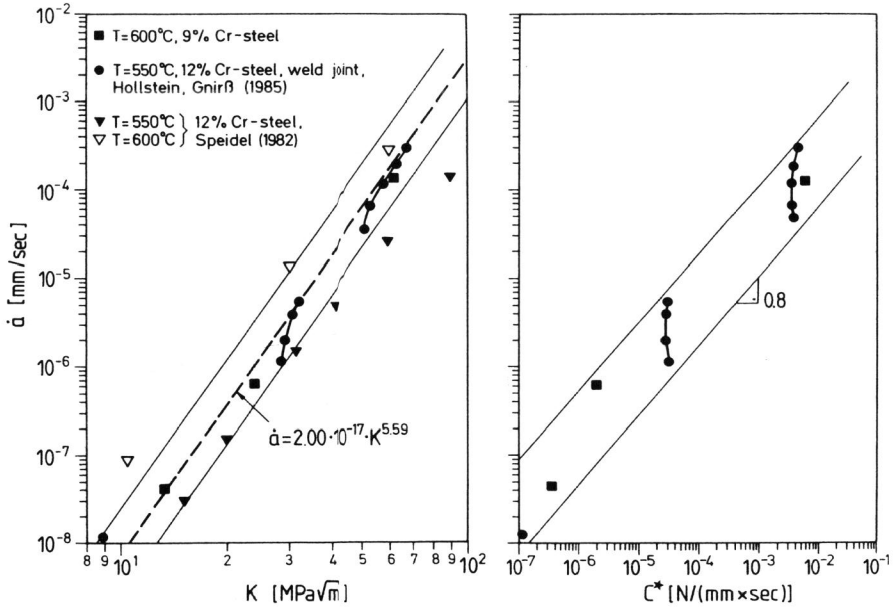

Fig. 8a: Creep crack growth rate $\dot{a}$ as a function of C*

Fig. 8b: Creep crack growth rate $\dot{a}$ as a function of C* integral

An example where creep crack growth undoubtedly is controlled by K is discussed by Riedel and Wagner (1984). They tested two different sizes of CT specimens of a nickel-base superalloy Nimonic 80 A. This alloy had a transition time t_1 of many years which exceeds significantly the transition time of the 9-12% Cr steels, shown in Fig. 8.

CONCLUSIONS

For a wide range of materials and testing conditions, the creep crack growth rate in tension and compact specimens with different sizes can be described - and hence predicted - by the fracture mechanics paramters C*, C_t, K and J, respectively, provided that certain limits of validity - described in detail by Riedel (1987) - were respected.

For two steels (18% Cr 6% Ni and 32% Ni 20% Cr) a C*-controlled region of steady-state creep crack growth could be shown to exist independent of geometry and size of specimens. The characteristic time t_1 was small in comparison to the failure time of specimen.

For the 32% Ni 20% Cr material, an increase in loading rate (specimen failure less than one day) showed a transition to J-controlled crack growth, where time independent plasticity predominates.

The limitation of C* due to crack tip blunting was demonstrated by experiments at 900°C with CN specimens of the alloy Inconel 617.

Effects of elasticity within a C*-controlled crack growth region were present in the 1% Cr steel tested. This was particularly obvious during the first stage of the lifetime of the specimen where crack growth was shown to be characterized by the stress intensity factor K. The transient behaviour and the dependencies on size, crack length and type of specimen could be explained by models.

K-controlled creep crack growth appeared to be present in the 9-12% Cr steels tested. Here, the characteristic time t_1 was of the order of the failure time of the specimen.

ACKNOWLEDGEMENT

The author is grateful to the Stiftung Volkswagenwerk, to the Deutsche Forschungsgemeinschaft, to the Bundesminister für Forschung und Technologie who supported parts of this work. He also wishes to thank Mr. U. Goerke for carefully performing the experiments.

REFERENCES

Ainsworth, R.A., Coleman, M.C. (1987). Fatigue and Fracture of Engineering Materials and Structures, 10, 129-140.

Ewald, J., Keienburg, K.H., Maile K. (1985). Nulcear Engineering and Design, 87, 389-398.

Ewald, K.H., Maile, K., Tscheuschner, R. (1987). In: 13. MPA-Seminar, 8./9. Oktober 1987, Band 2, 43.1-43.26.

Hollstein, T. (1986). Fracture Control of Engineering Structures, Proceedings of EDF 6, Vol. I, 451-461.

Hollstein, T., Webster, G.A., Djavanroodi, F., Holdsworth, S.R. (1988). In: Failure Analysis - Theory and Practice - ECF7, Vol. 2, 656-668.

Hollstein, T., Gnirss, G. (1985). In: Vorträge der 17. Sitzung des Arbeitskreises Bruchvorgänge, 79-100.

Hollstein, T., Kienzler, R. (1987). In: Vorträge der 19. Sitzung des Arbeitskreises Bruchvorgänge, 315-327.

Hollstein, T., Kienzler R. (1988). Journal of Strain Analysis, 23, 87-96.

Hollstein, T., Voss, B., (1986). Presented at Third Int. Symp. on Nonlinear Fracture Mechanics, Knoxville, to be published in ASTM STP.

Kloos, K.H. Granacher, J., Tscheuschner, R (1987). Z. f. Werkstofftechnik, 18, 390-398.

Kumar, V., German, M.D. and Shih, C.F. (1981). An Engineering Approach for Elastic-Plastic Fracture Mechanics Analysis, Report No. EPRI NP-1931, Research Projekct 1237-1, General Electric, Schenectady.

Landes, J.D. and Begley, J.A. (1976). In: Mechanics of Crack Growth, ASTM STP 590, 128-148.

Ohji, K., Ogura, K., Kubo, S. (1974). Preprint of Jap. Soc. Mech. Engrs., No. 640-11, 207.

Riedel H. (1987). Fracture at High Temperatures, Springer Verlag.

Riedel, H. and Rice, J.R. (1980). In: Fracture Mechanics, Twelfth Conference, ASTM STP 700, 112-130.

Riedel H., Wagner, W. (1984). In: Advances in Fracture Research '84, Proceedings of ICF 6, Vol.3, 2199-2206.

Rödig, M., Kienzler R., Nickel, H., Schubert, F. (1988). Nuclear Engineering and Design, 108, 467-476.

Saxena, A. (1986). In: Fracture Mechanics, Seventeenth Symposium, ASTM STP 905, 185-201.

Saxena, A., Landes, J.D. (1984). In: Advances in Fracture Reserach '84, Proceedings of ICF 6, Vol. 6, 3977-3988.

Shih, C.F., deLorenzi, H.G., Andrews, W.R. (1977). Int. Journ. of Fracture, 13, 544-548.

Speidel, M. (1982). Unpublished Results.

Webster, G.A., Smith, D.J., Nikbin, K.M. (1986). In: Proceedings Int. Conference on Creep, Tokyo, 303-308.

Webster, G.A. (1983). In: Engineering Approaches to High Temperature Design, Pineridge Press.

Yokobori, T., Yokobori Jr., A.T., Sakata, H., Maekawa, I. (1980). In: Proceedings of the IUTAM Symposium on three-Dimensional Consitutive Relations and Ductile Fracture, Dourdan, 365-386.

Yokobori Jr., Yokobori, A.T., Kurijama, T., Kao, T., Kaji, Y. (1987). In: Proc. of Int. Conf. on Creep, Tokyo, 135-140.